

# Contribution of Atmospheric Rivers to Antarctic Precipitation

Jan Thérèse Maria Lenaerts<sup>1</sup>, Michelle Laura Maclennan<sup>1</sup>, Christine A Shields<sup>2</sup>, and Jonathan D Wille<sup>3</sup>

<sup>1</sup>University of Colorado Boulder

<sup>2</sup>National Center for Atmospheric Research (UCAR)

<sup>3</sup>Université Grenoble Alpes

November 24, 2022

## Abstract

Atmospheric rivers (ARs) are efficient mechanisms for transporting atmospheric moisture from low latitudes to the Antarctic Ice Sheet (AIS). While AR events occur infrequently, they can lead to extreme precipitation and surface melt events on the AIS. Here we estimate the contribution of ARs to total Antarctic precipitation, by combining precipitation from atmospheric reanalyses and an polar-specific AR detection algorithm. We show that ARs contribute substantially to Antarctic precipitation, especially on East Antarctica at elevations below 3000 meters. ARs play a vital role in explaining the substantial year-to-year variability in Antarctic precipitation. Our results highlight that ARs are an important component for understanding present and future Antarctic mass balance trends and variability.

1  
2  
3  
4  
5  
6  
7  
8  
9  
10  
11  
12  
13  
14

# Contribution of Atmospheric Rivers to Antarctic Precipitation

Jan T. M. Lenaerts<sup>1,\*</sup>, Michelle L. Maclennan<sup>1,\*</sup>, Christine Shields<sup>2</sup>, Jonathan D. Wille<sup>3</sup>

<sup>1</sup>Department of Atmospheric and Oceanic Sciences, University of Colorado Boulder, Boulder CO, USA

<sup>2</sup>National Center for Atmospheric Research, Boulder CO, USA

<sup>3</sup>Institut des Géosciences de l'Environnement, Grenoble, France

\* These authors have contributed equally to the work

## Key Points:

- Atmospheric rivers (ARs) contribute around  $13\pm 3\%$  to Antarctic Ice Sheet (AIS) precipitation.
- The relative contribution of ARs to precipitation is most substantial in East Antarctica.
- ARs explain a large fraction (35%) of interannual variability in AIS precipitation.

---

Corresponding author: Jan T. M. Lenaerts, [Jan.Lenaerts@colorado.edu](mailto:Jan.Lenaerts@colorado.edu)

**Abstract**

Atmospheric rivers (ARs) are efficient mechanisms for transporting atmospheric moisture from low latitudes to the Antarctic Ice Sheet (AIS). While AR events occur infrequently, they can lead to extreme precipitation and surface melt events on the AIS. Here we estimate the contribution of ARs to total Antarctic precipitation, by combining precipitation from atmospheric reanalyses and an polar-specific AR detection algorithm. We show that ARs contribute substantially to Antarctic precipitation, especially on East Antarctica at elevations below 3000 meters. ARs play a vital role in explaining the substantial year-to-year variability in Antarctic precipitation. Our results highlight that ARs are an important component for understanding present and future Antarctic mass balance trends and variability.

**Plain Language Summary**

Antarctica is the driest continent on Earth. The rare snowfall events on the cold Antarctic desert usually come from so-called atmospheric rivers, the same type of systems that bring winter precipitation along the western coasts of the American continents, such as the Pacific Northwest in the United States. Here we estimate how much precipitation on Antarctica is associated with these atmospheric rivers. Even though they only occur a few days per year, atmospheric rivers explain around 13% of the total Antarctic precipitation. Even more importantly, we find a strong link between year-to-year variations in Antarctic precipitation and atmospheric rivers, underlining the importance of these systems for understanding current and future changes of the Antarctic ice sheet contribution to global sea level rise.

**1 Introduction**

The Antarctic Ice Sheet (AIS) is losing mass at an accelerated pace, with a tripling of mass loss ( $200 \text{ Gt yr}^{-1}$  or Gigatonnes ( $10^{12}$  kg) per year) in recent years (2012-2017) relative to the early 1990s (Shepherd et al., 2018; Rignot et al., 2019). On top of that multi-decadal AIS mass loss signal, which is primarily driven by ocean warming and subsequent ice shelf thinning and areal loss, and grounding line retreat, AIS mass balance varies substantially from year to year (Wouters et al., 2013; Rignot et al., 2019). These mass balance variations are determined by atmospheric processes, particularly snowfall, which is the primary input term of the AIS mass balance (Lenaerts et al., 2019). While

46 annual snowfall rates on AIS are generally low (<200 mm per year), a substantial por-  
47 tion of the annual snowfall is associated with highly episodic marine air intrusions (Nicolas  
48 et al., 2011; Maclennan & Lenaerts, 2021) or synoptic-scale cyclones (Dalaiden et al., 2020;  
49 Turner et al., 2019). Some of these systems generate long, narrow plumes of strong hor-  
50 izontal water vapor transport, referred to as atmospheric rivers (ARs; Zhu & Newell, 1998).  
51 While ARs are well known to impact certain mid-latitude regions, particularly the west  
52 coast of the American continents, recent work has highlighted their importance for ice  
53 sheet mass balance. For example, Mattingly et al. (2020) showed that atmospheric rivers  
54 in summer enhance surface melt and rainfall over the Greenland Ice Sheet. Wille et al.  
55 (2019) demonstrated that most surface melt events on the West Antarctic Ice Sheet are  
56 explained by ARs, as they bring relatively warm air masses from lower latitudes, some-  
57 times as far as the subtropics (Terpstra et al., 2021). As surface melt and rain on the  
58 AIS is generally limited to the ice shelves (Trusel et al., 2013; Johnson et al., 2021), and  
59 nearly all meltwater refreezes in the firn, ARs are currently more relevant for precipi-  
60 tation on the AIS. Considering that AR are likely to become more impactful in the fu-  
61 ture (Payne et al., 2020), and AIS precipitation is expected to increase (Dalaiden et al.,  
62 2020; Lenaerts et al., 2016), it is essential to better constrain ARs and their impact on  
63 contemporary AIS surface mass balance. In situ observations on the East Antarctic es-  
64 carpment have shown that ARs can contribute up to 80% of the annual snowfall (Gorodetskaya  
65 et al., 2014). In West Antarctica, seasonal surface height increases, as measured by satel-  
66 lite laser altimetry, can be attributed to unusually strong AR activity (Adusumilli et al.,  
67 2021). Most recently, Wille et al. (2021) used an AR detection algorithm to confirm that,  
68 while ARs only occur a few times per year along the Antarctic coastline, they contribute  
69 significantly to AIS snowfall especially in East Antarctica. A question that emerges from  
70 this previous work, in the framework of ongoing AIS mass loss, is: how much mass, in  
71 the form of precipitation, do ARs contribute to the AIS every year? Here we aim to ad-  
72 dress that question, using a combination of a polar-specific AR algorithm and reanal-  
73 ysis precipitation products. Section 2 discusses the data and methods used in this study.  
74 Section 3 presents the results, and Section 4 provides a discussion of our findings and  
75 conclusions.

## 2 Data and Methods

### 2.1 MERRA-2

In this work, we use output of the atmospheric reanalysis product MERRA-2 (Gelaro et al., 2017) from the National Aeronautics and Space Association (NASA). In particular, we use total (snowfall + rainfall) precipitation fields at three-hourly (for the AR precipitation, see below) and monthly time resolution (for the total). We included rainfall in our study, since it is very small over Antarctica (Vignon et al., 2021), and most rain water instantaneously refreezes in the cold firn, essentially implying that rainfall is an input term of the current Antarctic mass balance. Effects of rain on firn thermal and density structure are not accounted for in this study. MERRA-2 is selected because the snow accumulation (i.e. precipitation - sublimation) field over Antarctica compares most favorably to ice core accumulation records of multiple state-of-the-art reanalysis products (Medley & Thomas, 2019).

### 2.2 AR detection algorithm

To detect atmospheric rivers, we use the detection algorithm described in Wille et al. (2021), which uses the meridional component of the integrated water vapor transport (vIVT) fields between 37.5°S and 80°S from the MERRA-2 atmospheric reanalysis. ARs are delineated by anomalously high (>98th percentile) vIVT values, and redetermined every 3 hours. If a filament of anomalously high vIVT values extends continuously for at least 20° in the meridional direction, then it is identified as an AR. It is a participating algorithm in ARTMIP (Atmospheric River Tracking Method Intercomparison Project; (Shields et al., 2018; Rutz et al., 2019)) and differs from many ARDTs in that it is regionally specific to Antarctica, not a generalized global algorithm, and detects ARs at a lower frequency compared to other global algorithms. Following Wille et al. (2021), we use vIVT instead of integrated water vapor (IWV) for AR precipitation attribution, given that the meridional moisture transport better reflects the dynamical processes associated to ARs. The algorithm excludes areas south of 80°S, since the AR vIVT signal quickly dissipates in the high-elevation interior of Antarctica as the humidity of the boundary layer is often dominated by the katabatic flow (Gorodetskaya et al., 2014).

Next, we combine this AR detection catalogue with MERRA-2 snowfall, and we define AR associated precipitation as precipitation that falls directly within each AR foot-

107 print, as well as in the 24-hour ( $\pm 6$  hours) long period after an AR has made passage.  
108 This  $24 \pm 6$  hour period, which is also used in Wille et al. (2021) is selected after care-  
109 ful analysis of precipitation rates in MERRA-2 during and after AR passage across the  
110 AIS for year 2019 (Figure 1). For this analysis, we used an hourly version of the AR de-  
111 tection algorithm (Alison Collow, personal communication), which provides more tem-  
112 poral detail but uses the same vIVT threshold method compared to the original 3-hourly  
113 algorithm (see above). We focus on the time period after the last time step an AR was  
114 detected, so we did not account for those time steps after which an AR was still detected.  
115 This gives insight in how precipitation rates vary after AR passage, or, in other words,  
116 how long ARs continue to affect precipitation after they have passed by a certain loca-  
117 tion. The results are summarized for the entire AIS and per glacier drainage basin (Fig-  
118 ure 1), and show that precipitation rates quickly decline in the first  $\sim 10$  hours after AR  
119 passage, after which they the rate decline slows down. After 10 hours, precipitation rates  
120 have decreased to approximately half of the original, and after 20 hours to less than 40%.  
121 We decided to use 24 hours as a cut-off time, i.e. all precipitation before that time is con-  
122 sidered AR precipitation, while any precipitation after 24 hours is not. We chose for this  
123 because of two main reasons: (1) at around 24 hours, more than 80% of cumulative pre-  
124 cipitation has fallen since AR passage on average, and rates are decreasing only very slowly  
125 afterwards; (2) 24 hours is available in the 3-hourly AR catalogues we use in this study,  
126 and is transferable to studies for which only daily precipitation rates are available. To  
127 quantify the uncertainty associated to this choice, we use the standard deviation of the  
128 time step when 80% cumulative precipitation is reached in each glacier drainage basin  
129 (Figure 1), which equals  $\sim 6$  hours.

130 Next, we checked the validity of our choice with a slightly different approach, and  
131 using our original 3-hourly AR algorithm. We calculated the relative change in AIS-integrated  
132 AR precipitation with each 3-hourly increase in cut-off time (e.g. 3 hours only accounts  
133 for precipitation until 3 hours after passage to the AR precipitation). While the rela-  
134 tive increase initially increases steeply (e.g. 18% increase when using 6 hrs past AR pas-  
135 sage compared to using 3 hrs past AR passage), the relative increase between each 3 hr  
136 increase quickly lowers, and is lower than 5% after 18 hours. This remaining small in-  
137 crease with a later cut-off time is to be expected, and likely due to the residual AR-related  
138 moisture being incorporated in mesoscale cyclogenesis over the AIS, the impact of a new  
139 AR as part of a series of ARs passing by the same location, and/or the general occur-

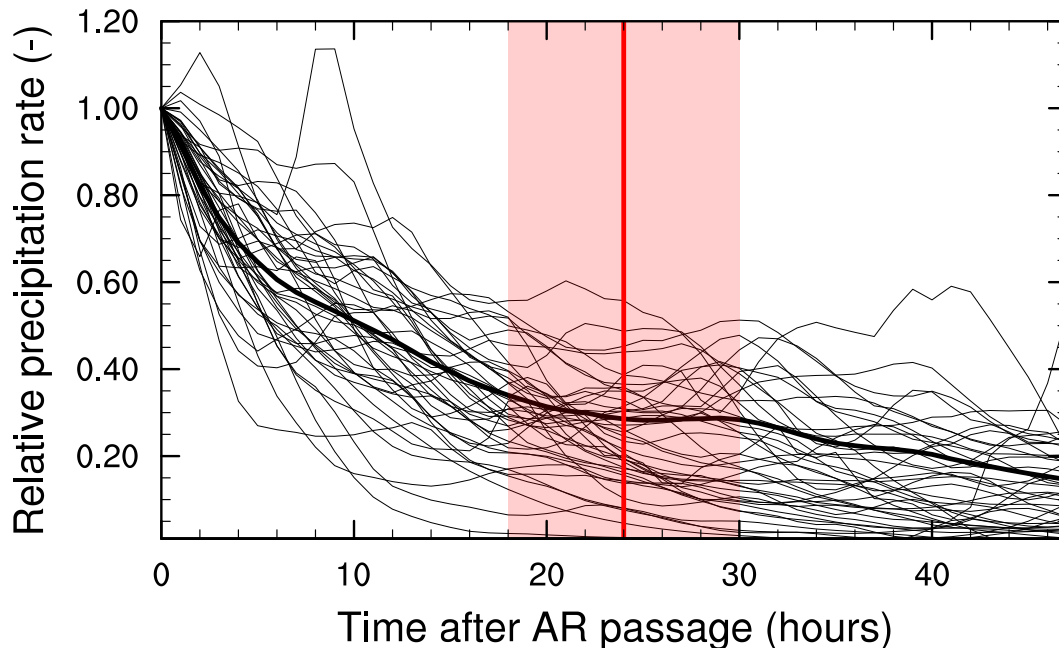


**Figure 1.** Mean precipitation rate as a function of time after AR passage, expressed relative to the last time step of AR passage, on the AIS for the year 2019. The thick black line denotes the mean of all ARs on the AIS, and the thin black lines show results for each individual glacier drainage basins (Shepherd et al., 2012). The vertical red line and shading show the  $24 \pm 6$  hr time window that we have selected as the most suitable period to present our AR precipitation results.

140    rence of AIS precipitation occurring outside the footprint of the detected ARs. This find-  
 141    ing validates our choice of  $24 \pm 6$  hour period, which likely includes most of the AR at-  
 142    tributed precipitation while excluding most precipitation from other sources.

### 143    **3 Results**

144        First we focus our analysis on the AIS-wide impact of ARs to precipitation. The  
 145        annual precipitation that can be attributed to ARs varies from less than 1 mm w.e. per  
 146        year on the Antarctic Plateau to  $>100$  mm w.e. per year on the low-elevation coastal  
 147        zones (Figure 3a). While total annual precipitation exhibits a similar gradient, with high  
 148        precipitation rates along the coast and very low precipitation rates in the interior (e.g.  
 149        Lenaerts et al., 2019), the relative contribution of ARs to that total precipitation is gen-  
 150        erally highest at lower elevations of the grounded ice sheet. The highest contributions  
 151        ( $>20$  %) are found in large parts of East Antarctica (Figure 3b), while relative contri-

152 contributions are lowest on the large Ross, Ronne-Filchner, and Amery ice shelves, and in the  
 153 high-elevation (>3000 m a.s.l.) interior. Remarkably, the relative contribution of ARs  
 154 is markedly lower in the entirety of West Antarctica (generally <10%) compared to East  
 155 Antarctica. Integrated over the full ice sheet (including ice shelves, and excluding areas  
 156 poleward of 80°S), the AR precipitation equals  $336 \pm 83 \text{ Gt yr}^{-1}$ , equivalent to a  $13 \pm 3\%$   
 157 of total precipitation (which equals  $2592 \pm 127 \text{ Gt yr}^{-1}$ ). The relative importance of AR  
 158 precipitation is slightly higher on the grounded ice sheet (13%) than on ice shelves (11%),  
 159 and higher on East Antarctica (16%) than on West Antarctica (9%) and the Antarctic  
 160 Peninsula (10%). These results imply that the relative impact of ARs on precipitation  
 161 is at least a magnitude higher than their frequency on the AIS, which does not exceed  
 162 1 to 1.5% (Wille et al., 2021).

163 Interannual variations in AR precipitation on the AIS are substantial, which is il-  
 164 lustrated by the high (25%) ratio between the 1980-2019 AR precipitation standard de-  
 165 viation and mean, in comparison to the 5% ratio for total precipitation. This is further  
 166 confirmed by the strong correlation (squared correlation coefficient  $R^2 = 0.96$ ) between  
 167 interannual variations of ice sheet integrated AR precipitation and its relative contribu-  
 168 tion to total AIS precipitation (Figure 3c). Detrended AIS AR precipitation and total  
 169 precipitation are moderately correlated (linear slope = 0.98;  $R^2 = 0.35$ ), indicating that  
 170 ARs can explain more than a third of the interannual variability in total AIS precipi-  
 171 tation, almost three times as much as ARs contribute to mean precipitation. Addition-  
 172 ally, we find that the relative contribution of ARs to total AIS precipitation displays a  
 173 small but discernible seasonal cycle (not shown), with a peak in winter and spring (>13.5%)  
 174 and a relative minimum (<12.5%) in summer (Dec-Feb). Considering the substantial in-  
 175 terannual variations, this seasonal cycle is nonetheless non-significant.

176 On top of these interannual variations, MERRA-2 suggests that total AIS precip-  
 177 itation has decreased during 1980-2019, albeit at a non-significant rate ( $-2.3 \pm 1.7 \text{ Gt yr}^{-2}$   
 178  $p=0.2$ ). AR precipitation, on the other hand, shows a clear and statistically significant  
 179 upward trend ( $2.5 \pm 1.1 \text{ Gt yr}^{-2}$ ,  $p=0.02$ ). The opposite long-term trends imply that the  
 180 relative contribution of ARs to AIS precipitation has increased towards the later years  
 181 of the time period (Figure 3), and relative AR contribution has increased substantially  
 182 ( $0.11 \pm 0.04 \text{ \% yr}^{-1}$ ,  $p < 0.01$ ), both for the grounded ice sheet and ice shelves. In 2009  
 183 and 2011, when multiple ARs hit the Dronning Maud Land area (Gorodetskaya et al.,  
 184 2014), the AR contribution exceeded 20%.

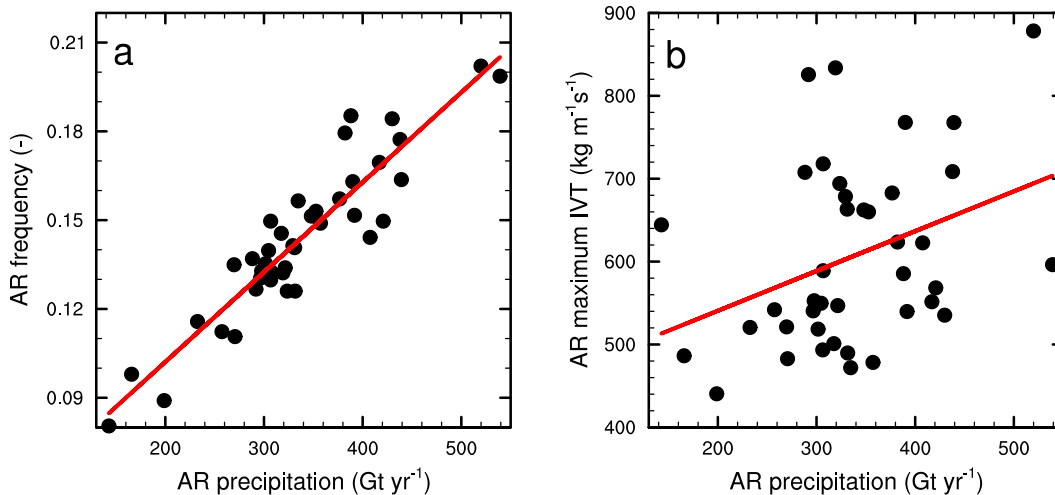


**Figure 2.** Annual AIS AR precipitation (1980-2019, horizontal axis) versus (a) annual AR frequency (1980-2019) on the AIS, defined here as the relative time an AR exists anywhere on the AIS; and (b) Annual mean (1980-2019) AR strength, approximated here by the mean IVT maximum found in all Antarctic ARs during each year.

185 An additional question emerging from our results is: what drives these variations  
 186 in AR precipitation on the AIS? Both interannual variability and long-term trend in AR  
 187 precipitation are strongly ( $R^2=0.85$ ,  $p<0.01$ ) correlated with the frequency of ARs on  
 188 Antarctica (Figure 2), indicating that years with more (less) ARs making landfall on AIS  
 189 are also associated with more (less) AR precipitation. However, we also find a small but  
 190 significantly positive ( $R^2=0.13$ ,  $p=0.02$ ) correlation between AR precipitation and the  
 191 annual average maximum IVT value in ARs on the AIS (Figure S1), suggesting a po-  
 192 tential link between the strength of ARs (as measured by IVT) on Antarctica and their  
 193 precipitation.

194 To further interpret the regional variability in the impact of ARs on Antarctic pre-  
 195 cipitation, we direct our analysis to individual glacier drainage basins. Figure 4a con-  
 196 firms that ARs contribute most to the total precipitation in the coastal East Antarctic  
 197 basins (basins 5-9 and 12-15), with contributions of 12 up to 20% (basin 8). The coastal  
 198 WAIS and interior EAIS basins show contributions of 10% and lower. Lowest AR con-  
 199 tributions to precipitation are found on Ross shelf ( $<5\%$ ), where AR frequency is also  
 200 lowest, but summer ARs have been shown to induce surface melt (Wille et al., 2019).  
 201 The spatial pattern in the extent to which ARs explain interannual variability (Figure

202 4b) largely reflects that of the AR contribution to the total, but the percentages are 3  
203 to 4 times higher in most basins. In the coastal EAIS basins, 60-75% of the variability  
204 in total precipitation is explained by ARs. Averaged across the EAIS, the explained vari-  
205 ance is 66%, substantially higher than the WAIS (55%) and the AP (34%).

206 While we found an overall positive trend in AR precipitation over the AIS, along  
207 with a small negative trend in total precipitation, these long term trends vary consid-  
208 erably from basin to basin (Figure 3c). In terms of total precipitation, we find strongly  
209 negative trends in Wilkes Land and western WAIS (basins 12 to 20), and overall pos-  
210 itive or negligible trends in other regions. AR precipitation trends are positive in most  
211 basins, and only negative in the western Wilkes Land region (basins 12-13). We find qual-  
212 itative agreement between the trend signs in most basins, suggesting that the long-term  
213 trends in AR precipitation partially explain the trends in total precipitation.

214 Finally, it is known that ARs, in part because of their remote, relatively warm source  
215 region and strong energetics, are able to penetrate deep in the interior of the ice sheet.  
216 We can validate this hypothesis using our results, as summarized in Figure 5. While the  
217 absolute precipitation rates associated to ARs clearly drop with elevation and distance  
218 to the coast (Figure 3a), their relative contribution to total precipitation remains remark-  
219 ably constant from the coast all the way to 3000 meters a.s.l.,. Above that elevation, the  
220 AR contribution drops sharply, but the associated uncertainties are large given that we  
221 have no data poleward of 80°S. Similarly, the contribution to total precipitation vari-  
222 ability remains constant from 0–3000 m a.s.l., and only slightly decreases above that el-  
223 evation. This signal is pretty consistent among different basins, despite inter-basin dif-  
224 ferences in values, and indicates that ARs are equally relevant to explaining annual ac-  
225 cumulation and its interannual variability in many interior, dry areas below 3000 m a.s.l.,  
226 where many ice cores are taken, compared to a low-elevation, maritime location.

## 227 4 Conclusions and Discussion

228 Our study combines an polar-specific AR detection algorithm with MERRA-2 pre-  
229 cipitation rates to quantify the contribution of ARs to Antarctic snowfall. We find that,  
230 integrated over the ice sheet, ARs contribute around 13% to Antarctic snowfall. The con-  
231 tribution varies substantially from year to year and on a regional (glacier basin) scale,  
232 but is relatively constant throughout the seasons and across elevation.

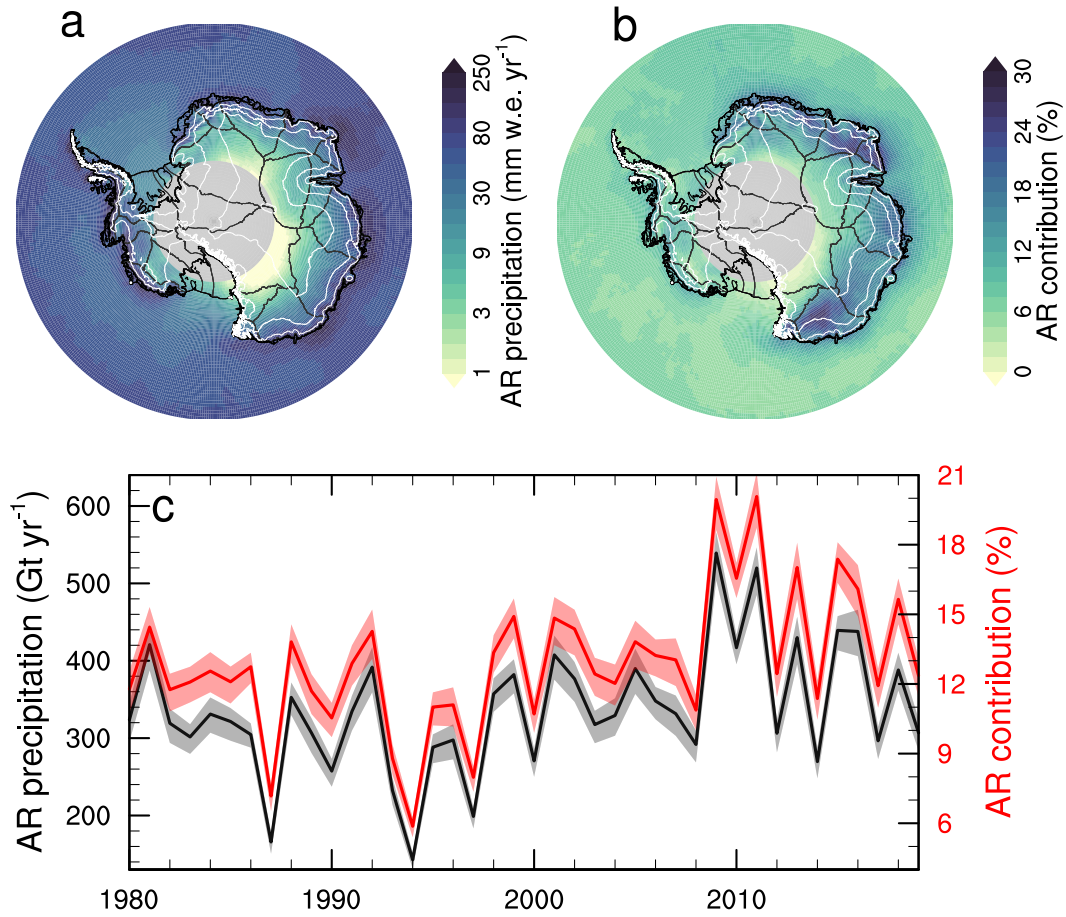


**Figure 3.** (a) 1980–2017 average precipitation attributed to ARs (mm w.e. per year); (b) 1980–2017 average relative contribution of AR precipitation (as shown in (a)) to the total annual precipitation; (c) Time series (1980–2017) of total AIS (grounded ice sheet and ice shelves) AR precipitation (black, in  $\text{Gt yr}^{-1}$ ), and relative contribution of AR precipitation to total precipitation (in red, in %). The delineations of the drainage basins that are used further in this study are shown in thin black lines, and the grounding line and ice shelf boundaries are shown in thicker black lines.

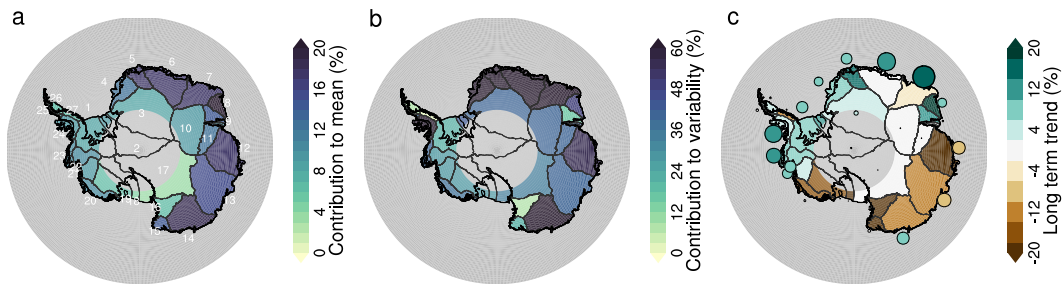


**Figure 4.** Relative contribution of AR precipitation to (a) the 1980–2019 average total precipitation; (b) the 1980–2017 interannual variability, defined as the percentage of explained variability of the best (positive) linear correlation between detrended annual AR and total precipitation; (c) the 1980–2019 relative change in total precipitation, with the dots showing relative change in AR precipitation (with same color scheme than total precipitation, and size proportional to relative change). Note that basins that are entirely poleward of  $80^{\circ}\text{S}$  are excluded in this analysis, but basins that partly cover  $>80^{\circ}\text{S}$  only include those areas  $<80^{\circ}\text{S}$ .

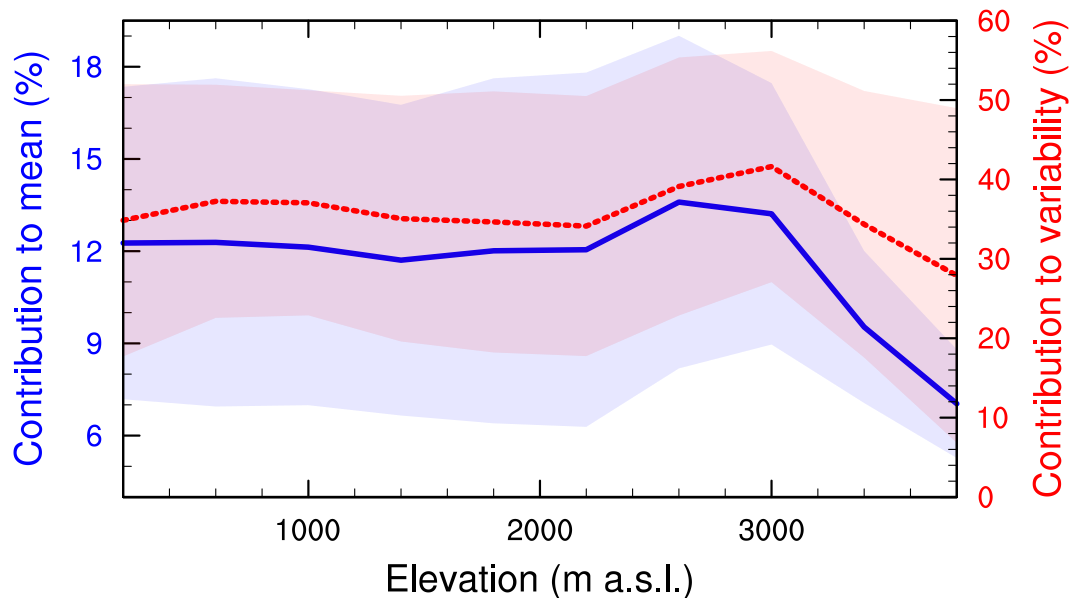


**Figure 5.** Relative contribution of AR precipitation to total precipitation (solid blue; left axis), and total precipitation variability (dashed red; right axis), as a function of elevation. The thick line shows the average of all basins, and the band indicates twice the standard deviation across all basins.

233 We acknowledge that substantial uncertainties are associated with our findings, par-  
234 ticularly as a result of our choice of AR detection algorithm and precipitation dataset.  
235 On the other hand, we have several reasons to believe that our estimates are likely con-  
236 servative. First of all, our precipitation product MERRA-2 is a global, gridded atmo-  
237 spheric reanalysis that does not assimilate but parameterizes precipitation rates and has  
238 a modest horizontal resolution (0.5 x 0.625 degrees). This likely leads to an underesti-  
239 mation of the highest precipitation rates, such as those associated to ARs, and thus an  
240 undercatch of the total precipitation assigned to an AR. Secondly, our assumed spatiotem-  
241 poral footprint of an AR on precipitation likely underestimates its real footprint. We only  
242 assign precipitation directly underneath an AR to that system, while in reality, the pre-  
243 cipitation field of an AR might be more expansive than that of the AR itself. The 24-  
244 hour time window after AR passage we use (and justify) might miss precipitation that  
245 persists for more than 24 hours after passage of strong AR systems (Wille et al., 2021).  
246 Thirdly, the AR detection algorithm used here is designed to capture high impact events,  
247 and likely misses weaker AR events more likely to be captured in global AR detection  
248 algorithms with lower thresholds. To further constrain ARs and their impact on Antarc-  
249 tica, future work should focus on using higher-resolution precipitation products (e.g. ERA5  
250 reanalysis, regional climate models), in conjunction with varied AR detection algorithms  
251 applied to that same product to estimate uncertainty based on the detection method.  
252 In addition, AR detection algorithm can be refined, for example by categorizing AR strength  
253 based on AR structure, size, vIVT threshold, and/or other conditions.

254 Current AR impacts in most regions of Antarctica are focused on snowfall, and thus  
255 ARs contribute positively to Antarctic surface mass balance. However, larger contribu-  
256 tions of ARs to snowfall in East Antarctica compared to West Antarctica suggest that  
257 that current AR impacts vary regionally. One hypothesis for this discrepancy is that West  
258 Antarctic ARs are less persistent, less meridionally expansive, and/or more of the 'windy  
259 and warm' rather than 'wet' type (Gonzales et al., 2020). Additionally, the zonal circu-  
260 lation around West Antarctica is better developed, and the position and strength of the  
261 Amundsen Sea Low, which is the dominant control of atmospheric circulation around  
262 West Antarctica (Turner et al., 2013), is extremely dynamic, both of which would limit  
263 the likelihood of the persistent atmospheric blocking needed for AR transport (Pohl et  
264 al., 2021). Further study is warranted to determine the AR flavors in different regions  
265 in Antarctica, and what impacts are associated to these different flavors. As global warm-

266 ing is likely to continue unabatedly in the future, leading to atmospheric temperature  
267 rise over Antarctica, AR strength and/or frequency might not only increase (Payne et  
268 al., 2020), but also their impact might shift. Particularly in the summer season and over  
269 coastal regions, ARs will bring enhanced potential of rainfall and surface melt at the ex-  
270 pense of snowfall, which affects firn properties (Kuipers Munneke et al., 2014) and ex-  
271 acerbates the risk for ice slab formation, meltwater ponding, runoff, and ice shelf hydrofrac-  
272 ture (Gilbert & Kittel, 2021). On the other hand, at higher elevations of the grounded  
273 ice sheet, ARs might bring even more enhanced snowfall in the future, aiding in miti-  
274 gating ocean-driven Antarctic mass loss.

### 275 **Acknowledgments**

276 J. T. M. Lenaerts acknowledges support from NASA (grant 80NSSC20K0888) and the  
277 National Science foundation (NSF, award 1952199). This work is from the the TARSAN  
278 project, a component of the International Thwaites Glacier Collaboration (ITGC). Sup-  
279 port from National Science Foundation (NSF: Grant 1929991) and Natural Environment  
280 Research Council (NERC: Grant NE/S006419/1). Logistics provided by NSF-U.S. Antarc-  
281 tic Program and NERC-British Antarctic Survey. ITGC Contribution No. ITGC-XXX.  
282 This material is based upon work supported by the U.S. Department of Energy, Office  
283 of Science, Office of Biological Environmental Research (BER), Regional and Global Model  
284 Analysis (RGMA) component of the Earth and Environmental System Modeling Pro-  
285 gram under Award Number DE-SC0022070 and NSF IA 1947282. This work was also  
286 supported by the National Center for Atmospheric Research (NCAR), which is a ma-  
287 jor facility sponsored by the NSF under Cooperative Agreement No. 1852977. C. Shields  
288 and M. Maclennan were partially supported under RGMA Award Number DE-SC0022070.  
289 M. L. Maclennan has also been supported by a NASA FINESST (grant 80NSSC21K1610).  
290 J. D. Wille acknowledges support from the Agence Nationale de la Recherche projects  
291 ANR-20-CE01-0013 (ARCA).

292 MERRA-2 precipitation data are available through the Goddard Earth Sciences  
293 Data and Information Services Center (hourly data at [https://disc.gsfc.nasa.gov/  
294 datasets/M2T1NXLF0.5.12.4/summary](https://disc.gsfc.nasa.gov/datasets/M2T1NXLF0.5.12.4/summary), monthly means at [https://disc.gsfc.nasa  
295 .gov/datasets/M2TMNXLF0.5.12.4/summary](https://disc.gsfc.nasa.gov/datasets/M2TMNXLF0.5.12.4/summary)).

296 The ARTMIP catalogues are available on the NCAR CGD gateway via [https://  
297 doi.org/10.5065/D6R78D1M](https://doi.org/10.5065/D6R78D1M). ARTMIP is a grass-roots community effort and includes

298 a collection of international researchers from universities, laboratories, and agencies. Co-  
 299 chairs and committee members include Jonathan Rutz, Christine Shields, L. Ruby Le-  
 300 ung, F. Martin Ralph, and Michael Wehner, Ashley Payne, Allison Collow, and Travis  
 301 O'Brien. Details on catalogues developers can be found on the ARTMIP website. ART-  
 302 MIP has received support from the US Department of Energy Office of Science Biolog-  
 303 ical and Environmental Research (BER) as part of the Regional and Global Climate Mod-  
 304 eling program, and the Center for Western Weather and Water Extremes (CW3E) at Scripps  
 305 Institute for Oceanography at the University of California, San Diego.

## 306 References

- 307 Adusumilli, S., A. Fish, M., Fricker, H. A., & Medley, B. (2021, 3). Atmospheric  
 308 River Precipitation Contributed to Rapid Increases in Surface Height of  
 309 the West Antarctic Ice Sheet in 2019. *Geophysical Research Letters*, *48*(5),  
 310 e2020GL091076. Retrieved from <https://doi.org/10.1029/2020GL091076>  
 311 doi: 10.1029/2020GL091076
- 312 Dalaiden, Q., Goose, H., Lenaerts, J. T. M., Cavitte, M. G. P., & Henderson, N.  
 313 (2020). Future Antarctic snow accumulation trend is dominated by atmo-  
 314 spheric synoptic-scale events. *Communications Earth & Environment*, *1*(1),  
 315 62. Retrieved from <https://doi.org/10.1038/s43247-020-00062-x> doi:  
 316 10.1038/s43247-020-00062-x
- 317 Gelaro, R., McCarty, W., Suárez, M. J., Todling, R., Molod, A., Takacs, L., ...  
 318 Zhao, B. (2017, 5). The Modern-Era Retrospective Analysis for Research  
 319 and Applications, Version 2 (MERRA-2). *Journal of Climate*, *30*(14), 5419–  
 320 5454. Retrieved from <https://doi.org/10.1175/JCLI-D-16-0758.1> doi:  
 321 10.1175/JCLI-D-16-0758.1
- 322 Gilbert, E., & Kittel, C. (2021, 4). Surface Melt and Runoff on Antarctic Ice  
 323 Shelves at 1.5°C, 2°C, and 4°C of Future Warming. *Geophysical Research*  
 324 *Letters*, *48*(8), e2020GL091733. Retrieved from [https://doi.org/10.1029/](https://doi.org/10.1029/2020GL091733)  
 325 [2020GL091733](https://doi.org/10.1029/2020GL091733) doi: 10.1029/2020GL091733
- 326 Gonzales, K. R., Swain, D. L., Barnes, E. A., & Diffenbaugh, N. S. (2020, 12).  
 327 Moisture- Versus Wind-Dominated Flavors of Atmospheric Rivers. *Geophysical*  
 328 *Research Letters*, *47*(23), e2020GL090042. Retrieved from [https://doi.org/](https://doi.org/10.1029/2020GL090042)  
 329 [10.1029/2020GL090042](https://doi.org/10.1029/2020GL090042) doi: <https://doi.org/10.1029/2020GL090042>

- 330 Gorodetskaya, I. V., van Lipzig, N. P. M., Claes, K., Tsukernik, M., Ralph, F. M.,  
331 Neff, W. D., ... van Lipzig, N. P. M. (2014, 9). The role of atmospheric rivers  
332 in anomalous snow accumulation in East Antarctica. *Geophysical Research*  
333 *Letters*, *41*(17), 6199–6206. Retrieved from [http://doi.wiley.com/10.1002/](http://doi.wiley.com/10.1002/2014GL060881)  
334 [2014GL060881](http://doi.wiley.com/10.1002/2014GL060881) doi: 10.1002/2014GL060881
- 335 Johnson, A., Hock, R., & Fahnestock, M. (2021). Spatial variability and re-  
336 gional trends of Antarctic ice shelf surface melt duration over 1979–2020  
337 derived from passive microwave data. *Journal of Glaciology*, 1–14. Re-  
338 trieved from [https://www.cambridge.org/core/article/spatial](https://www.cambridge.org/core/article/spatial-variability-and-regional-trends-of-antarctic-ice-shelf-surface-melt-duration-over-19792020-derived-from-passive-microwave-data/65A10CC1A103D0BF9CE7F9A3C08180AB)  
339 [-variability-and-regional-trends-of-antarctic-ice-shelf-surface](https://www.cambridge.org/core/article/spatial-variability-and-regional-trends-of-antarctic-ice-shelf-surface-melt-duration-over-19792020-derived-from-passive-microwave-data/65A10CC1A103D0BF9CE7F9A3C08180AB)  
340 [-melt-duration-over-19792020-derived-from-passive-microwave-data/](https://www.cambridge.org/core/article/spatial-variability-and-regional-trends-of-antarctic-ice-shelf-surface-melt-duration-over-19792020-derived-from-passive-microwave-data/65A10CC1A103D0BF9CE7F9A3C08180AB)  
341 [65A10CC1A103D0BF9CE7F9A3C08180AB](https://www.cambridge.org/core/article/spatial-variability-and-regional-trends-of-antarctic-ice-shelf-surface-melt-duration-over-19792020-derived-from-passive-microwave-data/65A10CC1A103D0BF9CE7F9A3C08180AB) doi: 10.1017/jog.2021.112
- 342 Kuipers Munneke, P., M. Ligtenberg, S. R., van den Broeke, M. R., van Angelen,  
343 J. H., & Forster, R. R. (2014, 1). Explaining the presence of perennial liquid  
344 water bodies in the firn of the Greenland Ice Sheet. *Geophysical Research*  
345 *Letters*, *41*(2), 476–483. Retrieved from [http://doi.wiley.com/10.1002/](http://doi.wiley.com/10.1002/2013GL058389)  
346 [2013GL058389](http://doi.wiley.com/10.1002/2013GL058389) doi: 10.1002/2013GL058389
- 347 Lenaerts, J. T. M., Medley, B., van den Broeke, M. R., & Wouters, B. (2019). Ob-  
348 serving and Modeling Ice Sheet Surface Mass Balance. *Reviews of Geophysics*,  
349 *57*, 376–420. doi: 10.1029/2018RG000622
- 350 Lenaerts, J. T. M., Vizcaino, M., Fyke, J., van Kampenhout, L., & van den Broeke,  
351 M. (2016). Present-day and future Antarctic ice sheet climate and surface  
352 mass balance in the Community Earth System Model. *Climate Dynamics*,  
353 *47*(5-6), 1367–1381. doi: 10.1007/s00382-015-2907-4
- 354 MacLennan, M. L., & Lenaerts, J. T. (2021, 9). Large-Scale Atmospheric Drivers  
355 of Snowfall Over Thwaites Glacier, Antarctica. *Geophysical Research Let-*  
356 *ters*, *48*(17), e2021GL093644. Retrieved from [https://doi.org/10.1029/](https://doi.org/10.1029/2021GL093644)  
357 [2021GL093644](https://doi.org/10.1029/2021GL093644) doi: 10.1029/2021GL093644
- 358 Mattingly, K. S., Mote, T. L., Fettweis, X., van As, D., Van Tricht, K., Lhermitte,  
359 S., ... Fausto, R. S. (2020). Strong Summer Atmospheric Rivers Trigger  
360 Greenland Ice Sheet Melt through Spatially Varying Surface Energy Bal-  
361 ance and Cloud Regimes. *Journal of Climate*, *33*(16), 6809–6832. Re-  
362 trieved from <https://journals.ametsoc.org/view/journals/clim/33/>

- 363 16/jcliD190835.xml doi: 10.1175/JCLI-D-19-0835.1
- 364 Medley, B., & Thomas, E. R. (2019). Increased snowfall over the Antarctic Ice Sheet  
365 mitigated twentieth-century sea-level rise. *Nature Climate Change*, 9(1), 34–  
366 39. doi: 10.1038/s41558-018-0356-x
- 367 Nicolas, J. P., Bromwich, D. H., Nicolas, J. P., & Bromwich, D. H. (2011, 1). Cli-  
368 mate of West Antarctica and Influence of Marine Air Intrusions\*. *Journal of*  
369 *Climate*, 24(1), 49–67. Retrieved from [http://journals.ametsoc.org/doi/](http://journals.ametsoc.org/doi/abs/10.1175/2010JCLI3522.1)  
370 [abs/10.1175/2010JCLI3522.1](http://journals.ametsoc.org/doi/abs/10.1175/2010JCLI3522.1) doi: 10.1175/2010JCLI3522.1
- 371 Payne, A. E., Demory, M. E., Leung, L. R., Ramos, A. M., Shields, C. A., Rutz,  
372 J. J., ... Ralph, F. M. (2020). Responses and impacts of atmospheric  
373 rivers to climate change. *Nature Reviews Earth and Environment*, 1(3),  
374 143–157. Retrieved from <https://doi.org/10.1038/s43017-020-0030-5>  
375 doi: 10.1038/s43017-020-0030-5
- 376 Pohl, B., Favier, V., Wille, J., Udy, D. G., Vance, T. R., Pergaud, J., ... Codron,  
377 F. (2021). Relationship Between Weather Regimes and Atmospheric Rivers  
378 in East Antarctica. *Journal of Geophysical Research: Atmospheres*, 126(24),  
379 e2021JD035294. Retrieved from <https://doi.org/10.1029/2021JD035294>  
380 doi: <https://doi.org/10.1029/2021JD035294>
- 381 Rignot, E., Mouginot, J., Scheuchl, B., van den Broeke, M., van Wessem, M. J., &  
382 Morlighem, M. (2019, 1). Four decades of Antarctic Ice Sheet mass balance  
383 from 1979–2017. *Proceedings of the National Academy of Sciences*, 116(4),  
384 1095 LP - 1103. Retrieved from [http://www.pnas.org/content/116/4/](http://www.pnas.org/content/116/4/1095.abstract)  
385 [1095.abstract](http://www.pnas.org/content/116/4/1095.abstract) doi: 10.1073/pnas.1812883116
- 386 Rutz, J. J., Shields, C. A., Lora, J. M., Payne, A. E., Guan, B., Ullrich, P., ...  
387 Viale, M. (2019, 12). The Atmospheric River Tracking Method Intercom-  
388 parison Project (ARTMIP): Quantifying Uncertainties in Atmospheric River  
389 Climatology. *Journal of Geophysical Research: Atmospheres*, 124(24), 13777–  
390 13802. Retrieved from <https://doi.org/10.1029/2019JD030936> doi:  
391 [10.1029/2019JD030936](https://doi.org/10.1029/2019JD030936)
- 392 Shepherd, A., Ivins, E., Rignot, E., Smith, B., Van Den Broeke, M., Velicogna,  
393 I., ... Wouters, B. (2018, 6). Mass balance of the Antarctic Ice Sheet  
394 from 1992 to 2017. *Nature*, 558(7709), 219–222. Retrieved from [http://](http://www.nature.com/articles/s41586-018-0179-yhttps://doi.org/10.1038/)  
395 [www.nature.com/articles/s41586-018-0179-yhttps://doi.org/10.1038/](http://www.nature.com/articles/s41586-018-0179-yhttps://doi.org/10.1038/)

- 396 s41586-018-0179-y doi: 10.1038/s41586-018-0179-y
- 397 Shepherd, A., Ivins, E. R., A, G., Barletta, V. R., Bentley, M. J., Bettadpur, S.,  
398 ... Zwally, H. J. (2012). A Reconciled Estimate of Ice-Sheet Mass Balance.  
399 *Science*, 338(6111), 1183–1189. doi: 10.1126/science.1228102
- 400 Shields, C. A., Rutz, J. J., Leung, L. Y., Martin Ralph, F., Wehner, M., Kawzenuk,  
401 B., ... Nguyen, P. (2018, 6). Atmospheric River Tracking Method In-  
402 tercomparison Project (ARTMIP): Project goals and experimental de-  
403 sign. *Geoscientific Model Development*, 11(6), 2455–2474. Retrieved  
404 from [https://gmd.copernicus.org/articles/11/2455/2018/https://](https://gmd.copernicus.org/articles/11/2455/2018/https://gmd.copernicus.org/articles/11/2455/2018/gmd-11-2455-2018.pdf)  
405 [gmd.copernicus.org/articles/11/2455/2018/gmd-11-2455-2018.pdf](https://gmd.copernicus.org/articles/11/2455/2018/gmd-11-2455-2018.pdf) doi:  
406 10.5194/gmd-11-2455-2018
- 407 Terpstra, A., Gorodetskaya, I. V., & Sodemann, H. (2021, 5). Linking Sub-  
408 Tropical Evaporation and Extreme Precipitation Over East Antarctica: An  
409 Atmospheric River Case Study. *Journal of Geophysical Research: Atmo-*  
410 *spheres*, 126(9), e2020JD033617. Retrieved from [https://doi.org/10.1029/](https://doi.org/10.1029/2020JD033617)  
411 [2020JD033617](https://doi.org/10.1029/2020JD033617) doi: <https://doi.org/10.1029/2020JD033617>
- 412 Trusel, L. D., Frey, K. E., Das, S. B., Munneke, P. K., & van den Broeke,  
413 M. R. (2013, 12). Satellite-based estimates of Antarctic surface melt-  
414 water fluxes. *Geophysical Research Letters*, 40(23), 6148–6153. doi:  
415 10.1002/2013GL058138
- 416 Turner, J., Bracegirdle, T. J., Phillips, T., Marshall, G. J., & Hosking, J. S.  
417 (2013, 3). An Initial Assessment of Antarctic Sea Ice Extent in the  
418 CMIP5 Models. *Journal of Climate*, 26(5), 1473–1484. Retrieved from  
419 <http://journals.ametsoc.org/doi/abs/10.1175/JCLI-D-12-00068.1>  
420 doi: 10.1175/JCLI-D-12-00068.1
- 421 Turner, J., Phillips, T., Thamban, M., Rahaman, W., Marshall, G. J., Wille, J. D.,  
422 ... Lachlan-Cope, T. (2019). The Dominant Role of Extreme Precipita-  
423 tion Events in Antarctic Snowfall Variability. *Geophysical Research Letters*,  
424 0(ja). Retrieved from <http://doi.wiley.com/10.1029/2018GL081517> doi:  
425 10.1029/2018GL081517
- 426 Vignon, , Roussel, M.-L., Gorodetskaya, I. V., Genthon, C., & Berne, A. (2021,  
427 4). Present and Future of Rainfall in Antarctica. *Geophysical Research Let-*  
428 *ters*, 48(8), e2020GL092281. Retrieved from <https://doi.org/10.1029/>

- 429 2020GL092281 doi: <https://doi.org/10.1029/2020GL092281>
- 430 Wille, J. D., Favier, V., Dufour, A., Gorodetskaya, I. V., Turner, J., Agosta, C.,  
431 & Codron, F. (2019). West Antarctic surface melt triggered by atmospheric  
432 rivers. *Nature Geoscience*, *12*(11), 911–916. Retrieved from [https://doi.org/](https://doi.org/10.1038/s41561-019-0460-1)  
433 [10.1038/s41561-019-0460-1](https://doi.org/10.1038/s41561-019-0460-1) doi: 10.1038/s41561-019-0460-1
- 434 Wille, J. D., Favier, V., Gorodetskaya, I. V., Agosta, C., Kittel, C., Beeman, J. C.,  
435 ... Codron, F. (2021, 4). Antarctic Atmospheric River Climatology and Pre-  
436 cipitation Impacts. *Journal of Geophysical Research: Atmospheres*, *126*(8),  
437 e2020JD033788. Retrieved from <https://doi.org/10.1029/2020JD033788>  
438 doi: 10.1029/2020JD033788
- 439 Wouters, B., Bamber, J. L., van den Broeke, M. R., Lenaerts, J. T. M., & Sas-  
440 gen, I. (2013, 8). Limits in detecting acceleration of ice sheet mass loss due  
441 to climate variability. *Nature Geoscience*, *6*(8), 613–616. Retrieved from  
442 <http://www.nature.com/articles/ngeo1874> doi: 10.1038/ngeo1874
- 443 Zhu, Y., & Newell, R. E. (1998). A Proposed Algorithm for Moisture Fluxes  
444 from Atmospheric Rivers. *Monthly Weather Review*, *126*(3), 725–735.  
445 Retrieved from [https://journals.ametsoc.org/view/journals/mwre/](https://journals.ametsoc.org/view/journals/mwre/126/3/1520-0493_1998_126_0725_apafmf_2.0.co_2.xml)  
446 [126/3/1520-0493\\_1998\\_126\\_0725\\_apafmf\\_2.0.co\\_2.xml](https://journals.ametsoc.org/view/journals/mwre/126/3/1520-0493_1998_126_0725_apafmf_2.0.co_2.xml) doi: 10.1175/  
447 [1520-0493\(1998\)126\(0725:APAFMF\)2.0.CO;2](https://journals.ametsoc.org/view/journals/mwre/126/3/1520-0493_1998_126_0725_apafmf_2.0.co_2.xml)